Transient heat transfer by free convection in a packed bed of spheres: Comparison between two modelling approaches and experimental results

Onrawee Laguerre, Sami Ben Amara, Graciela Alvarez, Denis Flick

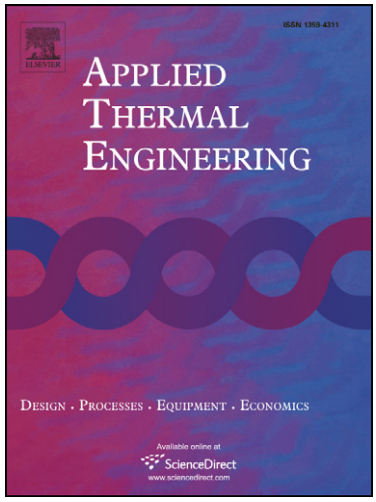

Transient heat transfer by free convection in a packed bed of spheres: Comparison between two modelling approaches and experimental results

O. Laguerre, S. Ben Amara, G. Alvarez, D. Flick

PII: S1359-4311(07)00100-7
DOI: 10.1016/j.applthermaleng.2007.03.014
Reference: ATE 2130

To appear in: *Applied Thermal Engineering*

Received Date: 20 October 2006
Revised Date: 23 January 2007
Accepted Date: 6 March 2007

Please cite this article as: O. Laguerre, S.B. Amara, G. Alvarez, D. Flick, Transient heat transfer by free convection in a packed bed of spheres: Comparison between two modelling approaches and experimental results, *Applied Thermal Engineering* (2007), doi: 10.1016/j.applthermaleng.2007.03.014

Transient heat transfer by free convection in a packed bed of spheres: Comparison between two modelling approaches and experimental results

O. Laguerre [a*], S. Ben Amara[a], G. Alvarez[a], D. Flick[b]

[a] UMR Génie Industriel Alimentaire Cemagref-ENSIA-INAPG-INRA, Cemagref, BP 44, 92163 Antony Cedex, France.

[b] UMR Génie Industriel Alimentaire Cemagref-ENSIA-INAPG-INRA, INAPG, 16 rue Claude Bernard, 75231 Paris, France.

Abstract

Two modelling approaches of transient heat transfer by free convection in a packed bed of spheres are carried out and then, compared with experimental results. The first approach uses computational fluid dynamics software which directly solves the Navier-Stokes equations and the local energy equations in the fluid and solid phases. It also includes radiation between the solid surfaces. The second approach, developed by the authors, uses methods developed for porous media and packed beds. The heat transfer model, based on a dispersed particle approach, takes into account air-particle convection, conduction and radiation between particles and 1-D-conduction inside the particles. The numerical results obtained using the two approaches are in good agreement with the experimental values of air and particle temperature for a particular free convection configuration.

Keywords: refrigeration, low air velocity, CFD simulation, packed bed modelling, natural convection, radiation.

[*] Corresponding author. Tel.:+331-4096-6121; fax:+331-4096-6075.
Email address: onrawee.laguerre@cemagref.fr

Symbols:

a	Thermal diffusivity, $m^2.s^{-1}$
a_v	Interface area per volume of packed bed, m^{-1}
C_1^*, C_2^*	Darcy and Forchheimer dimensionless coefficients
Cp	Heat capacity at constant pressure, $J.kg^{-1}.K^{-1}$
D	Particle diameter, m
$\boldsymbol{D}$	Total dispersion tensor, $m^2.s^{-1}$
$\boldsymbol{D^d}$	Dispersion tensor, $m^2.s^{-1}$
F	Empirical coefficient depending on porosity and microstructure of porous media
g	Gravitational acceleration, $m.s^{-2}$
h	Convective heat transfer coefficient, $W.m^{-2}.K^{-1}$
K	Permeability, m^2
k	Thermal conductivity, $W.m^{-1}.K^{-1}$
k_e	Effective thermal conductivity, $W.\ m^{-1}.K^{-1}$
n	Particle form factor
Nu	Nusselt number, $Nu = h.D/\lambda_{air}$
Nu_w	Nusselt number at wall, $Nu=h_w.D/\lambda_{air}$
p	Pressure, Pa
Pr	Prandtl number, $Pr = \mu/(\rho.a)$
r	Radial position, m
R	Radius of particle, m
Re	Reynolds number, $Re = \rho.u_{.}.D/\mu_{air}$
t	Time, s
T	Temperature, K

u	Fluid velocity, $m.s^{-1}$

Greece symbol

?	Density, $kg.m^{-3}$
e	Bed porosity
µ	Dynamic viscosity, Pa.s
µ'	Effective viscosity, Pa.s
ß	Thermal expansion coefficient, K^{-1}
s	Stefan-Boltzmann constant, s = 5.67040 x 10^{-8}, $W.m^{-2}.K^{-4}$
b	Thermal coefficient of volumetric expansion, K^{-1}

Subscript

cond	Conduction
rad	Radiation
e	Effective
eq	Equivalent
f	Fluid
p	Particle
p.s	Particle surface
0	Reference condition
m	Mean
s	Solid
w	Wall
∞	Reference condition

Introduction

Many transient heat transfer problems involve stacks of solid particles inside enclosures with heat exchanging walls. The fluid between the particles is then generally submitted to free convection. If the thermal conductivity and velocity of the fluid are low (in the case of free convection of air) and if the particle size is rather large (a few centimetres for a thermal diffusivity of the order of 10^{-7} $m^2.s^{-1}$ for example), the surface temperature of a particle can be significantly different from its core temperature over a long time interval (due to a low Fourier's number) and can also be very different from the fluid temperature (due to a low Biot number). The present study focuses particularly on this case, which is frequently encountered in the industry.

Free convection can take place in food process engineering, for example, fruit and vegetables chilled in a cold room or transported in a refrigerated truck. During their stay in these refrigerating equipments, the package walls exchange heat by convection with surrounding air and by conduction and radiation with food products. Of particular interest is the warming up of product when this one is stored in un-well-controlled ambience. Too high product temperature may lead to quality degradation (microbial growth or thawing). To minimize the quality losses, it is necessary to understand the heat transfer in the stack of product (considered as a packed bed) and this can be undertaken by modelling.

1. Approaches for heat transfer modelling

The modelling of heat transfer in a packed bed can be carried out by different approaches.

1.1. Direct Computational Fluid Dynamics (CFD) approach

The most direct approach to predict heat transfer and fluid flow in a packed bed is to numerically solve the Navier-Stokes equations and the local energy equations in the fluid and solid phases. The entire geometry of the system (solid and fluid phases) is meshed into elementary volumes. Different methods can be used to discretize the partial derivative equations on each elementary volume: finite element, finite volume…. The coupled non linear equations (heat, mass and momentum balances) are solved iteratively until a fixed convergence criterion is reached. This approach was first limited to 2-D geometry of few particles with laminar flow [1, 2]. With the increasing computing capacities, 3-D simulations are now possible. Several studies were carried out using CFD codes to simulate heat and mass transfers in packed bed [3-8]. For some models, the heat transfer through contact between the spheres is taken into account. A comparison between numerical and experimental results obtained by these studies shows that CFD can be an interesting tool to improve the understanding of fixed bed fluid flow and heat transfer. Logtenberg and Dixon (1998) [4] used a finite element code to simulate two layers of four spheres in laminar and turbulent flow ($9 < Re < 1450$). The k-ε model was used for turbulence. The mesh was composed of 30747 tetrahedral cells. They showed reasonable agreement for Nusselt number and effective thermal conductivity compared with experimental values. Romkes et al. (2003) [5] used CFD simulations to predict mass and heat transfer in a packed bed of 32 spheres, both in laminar and turbulent flow. The transfer rates were obtained with an average error of 15% compared with experimental data for Reynolds number (based on interstitial

velocity and hydraulic diameter) varying from 10^{-1} to 10^{5}. Magnico (2003) [6] studied numerically laminar fluid flow and mass transfer in a packed bed of several hundred of spheres. He presented a sensitivity study of meshing and solving parameters. Guardo et al. (2005) [7] compared the numerical prediction obtained with 5 turbulence models (Spalart-Almaras, standard k-e, RNG k-ε, realizable k-e, standard k-w) for a packed bed of 44 spheres. The best agreement with commonly used correlations was obtained with the Spalart-Almaras model which is less sensitive to the near-wall treatment. Guardo et al (2006) [8] extended this study for mixed (free + forced) convection.

Merrikh and Lage (2005) [9] used the CFD approach in the case of natural convection within up to 64 solid particles. They studied fluid flow and heat transfer in a differentially heated square enclosure with disconnected solids blocks. Two dimensional laminar simulations were performed for a Prandtl number equal to one, a Rayleigh number ranging from 10^{5} to 10^{8}, a fluid/solid thermal conductivity ratio from 0.1 to 100 and for different numbers (9 to 64) of solid blocks (constant fraction of volume occupied by the blocks: 36%). They found that where only a few solid blocks were used, the fluid flows predominantly along the channel between the heated (or cooled) wall and the first column of blocks. Where more numerous blocks were used, greater fluid flow occurs in some interior channels. This phenomenon is of great importance in terms of wall to fluid heat transfer.

CFD simulation is also largely used for many processes in food industry: sterilisation, drying, refrigeration. A review of studies using CFD in food industry was presented by Norton and Sun, 2006, [10]. For the simulation of transport phenomena in cold storage facilities, Tassou and Xiang, 1998 [11], Zou et al (2006), [12, 13] used CFD to predict the environmental conditions within ventilated packaging and cold room. Nahor et al

(2005) [14] used 2-phase modelling to predict cooling conditions within bulk containers.

1.2. Porous medium /packed bed approaches

In the direct CFD approach, each particle and interstitial space has to be meshed into thousands of cells; this requires extensive computational time even for a few hundred particles. Thus, the space-average methods developed for porous media and packed beds are more suitable for large stacks of particles. The fluid flow is then characterised by the superficial velocity (Darcy's velocity) which is a space average of the fluid velocity over a representative elementary volume [15, 16]. Fluid motion in porous media can be predicted by the general momentum equation of Darcy-Forchheimer-Brinkman [17].

$$\frac{?_0}{e}\left(\frac{\partial \vec{u}}{\partial t} + \vec{u}\cdot\vec{\nabla}\vec{u}\right) = -\vec{\nabla}p + ?\vec{g} + \frac{\mu'}{e}\nabla^2\vec{u} - \frac{\mu}{K}\vec{u} - r\frac{F}{\sqrt{K}}|\vec{u}|\vec{u} \qquad \textbf{(1)}$$

For packed beds of disordered spheres, Ergun's equation is often used [18]:

$$\vec{\nabla}p = -150\frac{(1-e)^2}{D^2e^3}\vec{u} - 1.75\frac{(1-e)}{De^3}|\vec{u}|\vec{u} \qquad \textbf{(2)}$$

This equation appears as a special case of Equation 1, in which the permeability and the Forchheimer coefficient are expressed as a function of porosity and particle diameter; some terms have been neglected (mechanical inertia and gravity are low for gaseous

fluids, Brinkmann stresses in the fluid and at the wall are negligible compared with friction with the particles for fluids of a low viscosity).

Generally, the heat transfer models in porous media consider the local thermal equilibrium between the fluid and solid phases. A single space-averaged temperature is then used which can be predicted by a convection-diffusion equation.

$$\left[e(?Cp)_f + (1-e)(?Cp)_s\right]\frac{\partial\langle T\rangle}{\partial t} + (?Cp)_f\,\vec{u}\cdot\vec{\nabla}\langle T\rangle = \vec{\nabla}\cdot\left(k_e\cdot\vec{\nabla}\langle T\rangle\right) + (?Cp)_f\,\vec{\nabla}\cdot\left(e\boldsymbol{D^d}\cdot\vec{\nabla}\langle T\rangle\right) \quad \textbf{(3)}$$

k_e is an effective thermal conductivity depending on fluid and solid conductivity, porosity and solid structure. D^d is an effective diffusion tensor depending on fluid velocity and taking into account the axial and radial fluid dispersion due to the solid obstacles [17]. An equivalent thermal conductivity is sometimes introduced in order to take into account the radiation between particles.

In the presence of heat generation in the solid phase or for transient problems, the local thermal equilibrium hypothesis is not well verified, especially for large particles and low-conductivity fluids. Thus, two-temperature models were derived, by homogenization methods involving space-averaged values over each phase [19]. These models require the determination of 2 effective conductivities, 4 effective diffusion tensors and a convective heat transfer coefficient between the two phases.

$$\frac{\partial\langle T\rangle^f}{\partial t} + \vec{u}_{ff}\cdot\vec{\nabla}\langle T\rangle^f + \vec{u}_{fs}\cdot\vec{\nabla}\langle T\rangle^s = \vec{\nabla}\cdot D_{ff}\cdot\vec{\nabla}\langle T\rangle^f + \vec{\nabla}\cdot D_{fs}\cdot\vec{\nabla}\langle T\rangle^s + \frac{A_{sf}}{V_f(?Cp)_f}h_{sf}\left(\langle T\rangle^s - \langle T\rangle^f\right) \quad \textbf{(4)}$$

$$\frac{\partial\langle T\rangle^s}{\partial t} + \vec{u}_{sf}\cdot\vec{\nabla}\langle T\rangle^f + \vec{u}_{ss}\cdot\vec{\nabla}\langle T\rangle^s = \vec{\nabla}\cdot D_{sf}\cdot\vec{\nabla}\langle T\rangle^f + \vec{\nabla}\cdot D_{ss}\cdot\vec{\nabla}\langle T\rangle^s + \frac{A_{sf}}{V_s(?Cp)_s}h_{sf}\left(\langle T\rangle^f - \langle T\rangle^s\right) \quad \textbf{(5)}$$

More empirical two-temperature models were proposed for packed beds [20] focusing on the main phenomena. For example, Schumann's model considers only convection in the fluid phase (no conduction or dispersion) and interface heat transfer depending on fluid velocity. Two-temperature models have been widely used in food process engineering, including heat generation (respiration of vegetables), mass transfer (dehydration) and packaging effects [14, 21, 22].

Nevertheless, in some transient problems, the two-temperature approach is inadequate because the centre and surface temperatures of a particle are significantly different. In other words, the heat transfer resistance inside the particle is not negligible. Dispersed-particle-based models are then used. In each representative elementary volume, they consider an average temperature for the fluid and a solid phase which depends on the radial position in the particles. The Dispersion-Concentric Model [23], for example, takes into account one-directional fluid flow with axial dispersion, convective heat transfer between the fluid and the particle's surface and radial conduction inside the particles. This model was used, for example, for nuclear debris beds [24]. Three-dimensional formulations were also proposed using Ergun's equation for fluid flow prediction. Xu and Burfoot (1999) [25] used this approach to model bulk storage of foodstuffs. They included moisture transfer, assuming radial diffusion inside the particles. Moisture and temperature predictions were compared with experimental data for a packed bed of potatoes cooled down by forced convection (one-directional flow).

This paper presents a comparison between experimental data and two modelling approaches for transient heat transfer by free convection in a packed bed of spheres. The

first approach uses computational fluid dynamics software (Fluent) which directly solves the Navier-Stokes equations and the local energy equations in the fluid and solid phases, including radiation between the solid surfaces. This approach requires extensive computational time since each sphere and interstitial space was meshed in thousands of cells. The second approach, proposed by the authors, uses methods developed for packed beds. The Darcy-Forchheimer (generalised Ergun's equation) was solved to predict the space-averaged (superficial) velocity. A Dispersed Particle based model was used for the heat transfer. This model, initially employed for 1-D forced convection flow, was extended to predict 2-D (or 3-D) natural convection. It takes into account conduction and radiation between the particle surfaces, which are not negligible in free convection. The programme was written in Matlab^{R} language.

To highlight the specificity of our work compared to that of the commercial CFD, first, the packed bed modelling approach is detailed. Then, the configuration used for the comparison is presented: experimental conditions, methods of measurement and simulation conditions (meshing, boundary conditions…). Finally, the experimental and numerical data obtained from the two approaches are compared.

2. Packed bed modelling approach (PBA)

2.1. Transport phenomena

Figure 1 presents the different phenomena taken into account. Some assumptions are made to simplify the problem when the fluid is air and the temperature differences are only few degrees (conditions encountered in many practical situations).

- For free convection flow, the Boussinesq approximation is used since the relative density variation is small. A linear relation between air density and air temperature, $\rho = \rho_\infty\{1-\beta(T-T_\infty)\}$, is used for the gravity term whereas a constant density (r_∞) is used in the other terms.
- Convective heat transfer between the fluid and the particle surface and between the fluid and the walls depends on the local superficial velocity.
- The thermal fluid inertia is negligible compared with the particle inertia. $\frac{e.r_f.Cp_f}{(1-e).r_s.Cp_s} << 1$
- Conduction occurs between adjacent particles and between particles and wall.
- Radiation occurs between the surfaces of particles and of the wall. The fluid does not contribute to radiation (transparent fluid). The radiative exchange expressions can be linearized since the temperature differences between walls are small compared with the average absolute temperature. Only the radiation between the surfaces of adjacent particles is considered.
- Radial conduction occurs in each particle.
- Mass transfer (water evaporation for example) is not taken into account.

2.2. Governing equation

The distributed state variables are:

- the superficial (or Darcy) velocity $\vec{u}(\vec{x},t)$ where $\vec{x}$ = (x,y,z) is the position in the packed bed,
- the space-averaged fluid temperature $T_{air}(\vec{x},t)$,

- the product temperature $T_p(\vec{x},r,t)$ where $\vec{x}$ is the position of the particle in the packed bed and r is the radial position inside the particle.

The surface temperature of a particle will be noted as: $T_{p.s}(\vec{x},t) = T_p(\vec{x},R,t)$, R being the outer radius of the particle.

2.2.1. Momentum

The Darcy-Forchheimer equation, including a buoyancy term, coupled with the continuity equation was used.

$$\vec{\nabla} \cdot \vec{u} = 0 \qquad \textbf{(6)}$$

$$\vec{\nabla} p = -C_1^* \frac{\mu}{D^2}\vec{u} - C_2^* \frac{?}{D}|\vec{u}|\vec{u} - ?_m ß(T_{air} - T_m)\vec{g} \qquad \textbf{(7)}$$

where r_m is the air density at the mean temperature T_m and b is the thermal expansion coefficient (Boussinesq approximation).

C_1^* and C_2^*, the Darcy and Forchheimer dimensionless coefficient can be found in the literature for packed beds [26, 27, 28].

2.2.2. Radial heat conduction inside the particles

$$r_p Cp_p \frac{\partial T_p}{\partial t} = \frac{1}{r^n}\frac{\partial}{\partial r}\left(k_p r^n \frac{\partial T_p}{\partial r}\right) \qquad \textbf{(8)}$$

where n is a particle form factor varying from 1 to 2 (1 for long cylinders, 2 for spheres).

2.2.3. Heat balance on the particle surface

Equation 9 represents the heat balance on the surface of the particles per unit volume of packed bed.

$$a_v k_p \left(\frac{\partial T_p}{\partial r} \right)_{r=R} = a_v h \left(T_{air} - T_{p.s} \right) + k_{eq} \nabla^2 T_{p.s} \qquad \textbf{(9)}$$

where a_v is the interface area per unit volume of packed bed.

The first term is the conductive heat flux inside the particles from the surface towards the core.

The second term is the convective heat exchange with air. The convective heat transfer coefficient h depends on superficial velocity and can be obtained from correlations between Nusselt and Reynolds numbers in packed beds [20, 29].

The third term takes into account the conductive and the (linearized) radiative exchanges between the particle surfaces. The equivalent thermal conductivity, k_{eq}, depends on fluid and solid thermal conductivity, particle arrangement and surface emissivity. Many correlations for the effective thermal conductivity of porous media were proposed in the literature using the one-temperature model [17]. However, they are

not valid when predicting the equivalent thermal conductivity introduced in this dispersed particle based model which holds only for the exchange between the surfaces of the particles. Ben Amara et al. (2004) [28] proposed an experimental characterisation of conductive and radiative exchanges for a cubic arrangement of spheres.

2.2.4. Convective heat balance for the fluid

Equation 10 takes into account the fact that the fluid warms up when it flows through warmer particles.

$$e.r_f.Cp_f \frac{\partial T_{air}}{\partial t} + \vec{\nabla} \cdot (?_m CpT_{air} \vec{u}) = a_v h(T_{p.s} - T_{air}) \quad \textbf{(10)}$$

In this equation, the first term corresponding to the thermal inertia was neglected because the thermal characteristic time of air is much higher than the one of spheres.

2.3. Boundary conditions

On the walls, the normal velocity is zero and tangential wall stress is neglected compared with the drag forces exerted by the particles. The Darcy and Forchheimer dimensionless coefficients can eventually be modified near the wall to take into account higher porosity (channelling effect).

Conductive and radiative exchanges occur between the walls and the adjacent particles in the same manner as in the bulk of particles: the wall temperature replaces the product surface temperature in Equation 9 at the boundary. If surface emissivity of the wall is

different from the particle emissivity, for example, the value of the equivalent thermal conductivity can be modified near the wall.

Convective exchanges occur between the cavity wall and the fluid in the same manner as that with the particle surface, but the heat transfer coefficients are different. Laguerre et al. [30] experimentally characterized these transfers for a wall bounded by a cubic arrangement of spheres.

2.4. Numerical resolution

A specific programme was developed to solve the set of partial differential equations. The finite volume method was used for spatial discretization. *Figure 2* shows the general algorithm which involves several iterative loops at each time step.

Conduction inside the product (Equation 8) is first solved by an explicit method allowing the prediction of the new product temperatures (except at the surface). The time step is automatically calculated in order to ensure the stability of this explicit method.

The pressure and the superficial velocity are then predicted by successive linearization of the Darcy-Forchheimer equation coupled with the continuity equation (Equations 6 and 7). The buoyancy source term is evaluated from the last estimated air temperature.

A new temperature field for air is then predicted using the previously estimated velocity and the last estimated surface temperature of the product. In order to achieve this, the heat balance for the fluid (Equation 10) is solved with an implicit upwind scheme.

Finally a new estimation of the surface temperature of the product is obtained from Equation 9.

3. The configuration investigated

3.1. Experimental device and measurements

The experimental device (*Figure 3*) is a parallelepiped enclosure containing 6 x 6 x 5 spheres, 7.5 cm in diameter, in cubic arrangement. Hollow spheres made of PVC were filled with an aqueous gelatine gel (96% water, 4% FlenogenM53). The upper, lower and side walls were insulated using extruded polystyrene (5 cm thickness, thermal conductivity 0.028 $W.m^{-1}.K^{-1}$). One of the vertical walls was made of aluminium (2 mm thickness) and exposed to the ambient air of a controlled temperature room (20°C). The other vertical wall was an aluminium plate in which a water-glycol mixture at a controlled temperature (0°C) can circulate.

The temperature at the centre of the spheres located on the symmetry plane was measured using calibrated thermocouples (Type T). The air temperature was measured in the pores at 9 locations (*Figure 3*) by placing thermocouple at the pore centre. Since the diameter of thermocouples (1 mm) is very small compared to the hydraulic pore diameter of the pores (4.5 cm), it was supposed that the effect of thermocouple on flow

pattern is negligible. The temperature of the two vertical walls was measured at three height levels (top, middle and bottom). Initially, the air and product were in equilibrium with the room temperature of 20°C (no refrigerant circulation). The water-glycol mixture was then circulated and the temperature of the left vertical wall decreased rapidly to reach an almost constant temperature of 0°C (cooling loop temperature). The total duration of the experiment was 10 000 min; it was observed that the steady state was achieved after 5000 min. The Rayleigh number in the cavity was approximately 2.3 x 10^8; calculation was based on the temperature of the warm and cold walls and its height. For the cavity loaded with spheres, the porous medium Rayleigh number is still lower so that the laminar flow regime is assumed.

3.2. Modelling with the packed bed approach

The correlation obtained for a cubic arrangement of spheres exposed to low air velocity proposed by [28, 29, 30] were used.

For the Darcy-Forchheimer equation (eq. 7):

$$\vec{\nabla} p = -C_1^* \frac{\mu}{D^2}\vec{u} - C_2^* \frac{?}{D}|\vec{u}|\vec{u} - ?_m ß(T_{air} - T_m)\vec{g}$$

C_1^* = 507 and C_2^* = 3.66 (for Re ≤ 450).

For convective heat transfer from particle surface to air:

$$Nu = 1.09\ Pr^{1/3}\ Re^{0.53} + 2 \qquad \textbf{(11)}$$

For Re ≤ 400 and Pr ≈ 0.71

For convective heat transfer from wall to air (in presence of the spheres):

$$Nu_w = 1.56\ Pr^{1/3}\ Re^{0.42} \quad \textbf{(12)}$$

For conductive and radiative heat transfer between the spheres (emissivity ≈ 1)

$$k_{eq} = k_{cond} + k_{rad} \quad \text{with} \quad \frac{k_{cond}}{k_{air}} = 2.09\left(\frac{k_p}{k_{air}}\right)^{0.32} \quad \text{and} \quad \frac{k_{rad}}{Ds\,T_m^3} = 2.15 \quad \textbf{(13)}$$

$$\text{For } 20 \le k_p/k_{air} \le 8000 \qquad \text{and} \qquad \Delta T/T_m \le 0.05$$

Where T_m is a mean temperature value: the final cold wall temperature was used (0°C).

The same parameters (C_1^*, C_2^*, k_{eq}) were used near the walls.

The equations were solved for the spheres located on the symmetry plane and the surrounding air. A regular cartesian mesh was used in which each cell contains one sphere ($Dx = Dy = D$). For each cell, the pressure, the horizontal and vertical superficial velocity components and the air temperature were calculated for each time step. Each sphere was divided into 5 concentric shells for which the product temperature was also calculated at each time step. The programme was written in Matlab^R language.

For the horizontal insulated walls, a Cauchy boundary condition was imposed. The external temperature was known (20°C) and the overall heat transfer coefficient of 0.54 $W.m^{-2}.K^{-1}$ was estimated. For the vertical walls, a Dirichlet boundary condition was imposed using the interpolated experimental data. Heat losses through the side walls were neglected, this allows two-dimensional resolution.

3.3. Modelling with the direct CFD approach

No correlation is needed for the direct CFD approach because velocity and temperature are directly calculated into the boundary layers near the walls and the product items. Boussinesq approximation was used for buoyancy. Radiation between all the wall and particle surfaces was taken into account by the discrete ordinate method [31].

The equations were solved 3-dimensionally using the CFD software Fluent 6.1.18 which uses the finite volume method of discretization The geometry has been constructed with tetrahedral cells following the bottom-up technique (generating surfaces and volumes from nodes and edges). *Table 1* presents the main solving parameters.

Taking advantage of symmetry, only a half of the enclosure was meshed. *Figure 4* presents the mesh which involves 189,124 cells for the solid spheres (9.51×10^6 cells/m^3 of solid) and 214,495 cells for the air void (1.19×10^7 cells/m^3 of void space). Considering the fluid phase around one sphere, the ratio between the mean cell volume and the void space is 1/2400. This ratio is the same order as the one used in other cited studies [4-6]. A slightly coarser mesh was also used and gave similar results.

The same boundary conditions as for the packed bed approach were used, but the heat transfer through the side walls was dealt with in the same manner as the horizontal walls.

4. Results and discussion

Figure 5 compares the measured and predicted product and air temperatures after 500 min, which corresponded to the transient state, and after 10 000 min (7 days), when the steady state was reached.

For both modelling approaches, the predictions are in relatively good agreement with the experimental data. *Figure 6* presents the mean error of prediction $\overline{|T_{measured} - T_{predicted}|}$ for air temperature and solid temperature (in the centre of the spheres). Overall, the packed bed approach gives better results than the direct CFD approach.

In fact, predictions are more or less accurate depending on the locations. *Figures 7a* and *7b* show an example of comparison between the experimental air and product temperature evolution with the results obtained by CFD and packed bed approaches.
The difference between the results of the 2 models and those of experiment (*Figure 5, 6 and 7*) may be due to:

- The simplifying assumption made in packed bed approach: heat losses through the side walls were neglected, wall shear stress was neglected compared to the drag forces exerted by the particles…
- In spite of the high number of cells (214495 cells) used in the CFD approach, the contact zones between spheres or between spheres and walls was difficult to mesh As in the study of Guardo et al (2006) [8], the spheres were modelled overlapping (1 mm overlap between spheres). In contrary, a 1 mm space between spheres and walls was used to allow better boundary layer development near the exchanging walls.

The 1 mm overlap or gap is very small (~1%) compared to the diameter of spheres (7.5 cm). It was therefore supposed that the results are not significantly influenced by this effect. A finer meshing may improve the CFD results. Manico (2003) [6] recommended a spatial resolution (grid size/particle diameter) of 1/40 which is lower than the value used in our study (~1/20).

- The precision of temperature measurement (±0.2°C).
- Both the air temperature presented by the CFD simulation and the experiment correspond to a pore centre (surrounded by spheres) whereas the one presented by the packed bed approach is an average for a pore volume.

The temperature profiles between the centre and surface of a sphere in a transient state was calculated by the packed bed approach (*Fig. 8*). It can be observed that the difference between the centre and surface temperatures can not be neglected.

Figure 9 compares the experimental and numerical temperature fields on the symmetry plane after 500 min. At 500 min, the first column of spheres located near the cold (left) wall began to cool down. Thermal stratification was observed: the coldest air and spheres are located near the bottom. The spheres and the surrounding air located near the warm (right) wall were still close to their initial temperature (20°C).

When steady state is reached, the observations are similar to the classical case of a differentially heated two-dimensional cavity. However, the thermal stratification (lower temperature near the bottom) is less pronounced than for an empty cavity because of the conductive and radiative exchanges through the solid phase. Indeed, if only conduction would occur, the isotherms would be vertical.

Figure 10 presents the predicted velocity fields when steady state is reached. For the packed bed approach, the (space averaged) superficial velocity is shown, whereas for the direct CFD approach, the local velocity vectors (on the plan located at 15.35 cm from the side wall where air occupies all the section) are shown. It is difficult to compare them directly; nevertheless it can be observed that airflow is weak near the centre of the enclosure. For the direct CFD approach, channelling effects are observed as mentioned by [6] for a similar case. The measurement of air velocity in the void for the box completely filled with spheres is difficult to do in practice. This explains the absence of the experimental values of air velocity which would be interesting to directly validate the numerical velocity results.

5. Conclusions

Two modelling approaches of transient heat transfer by free convection in a packed bed of spheres were compared with experimental results. A specific case was studied in which the temperatures of the core of a particle, of its surface and of the surrounding fluid can be significantly different. This kind of situation is frequently encountered in practice, for example in fruit and vegetable refrigeration. In this case, numerous numbers of fruits and vegetables (> 1000) are presents in cold room. In the direct CFD approach, the Navier-Stokes equations and the local energy equations in the fluid and solid phases (including radiation) are solved. Only the product geometries and properties are needed. But, each particle and interstitial space has to be meshed in thousands of cells and difficulties appear to mesh the product contact points. This approach requires extensive computational time and is therefore limited to several

hundreds of product items. To avoid the problems related to the direct CFD approach cited previously, a packed bed approach was thus developed. In this approach, the Darcy-Forchheimer equation is solved in order to predict the superficial velocity. The proposed heat transfer model, based on a dispersed particle approach, includes conduction and radiation between particles. These transfers are not negligible in free convection. The specific software developed in this study requires much less computational time than the CFD approach. This approach does not predict the details of the fluid flow and temperature at the pore scale, but only mean values on a representative elementary volume. Nevertheless, such information is generally not useful for applications. Finally, the packed bed approach could be applied to practical problems involving thousands of particles. The main limitation of this approach is the need of correlations for fluid flow resistance and heat transfer coefficients which are specific to a given geometry.

References

[1] M.T. Dalman, J.H. Merkin, C. McGreavy, Fluid flow and heat transfer past two spheres in a cylindrical tube, *Computational Fluids*, 14 (3) (1986), 267-281.

[2] B. Lloyd, R. Boehm, Flow and heat transfer around a linear array of spheres, *Numerical Heat Transfer*, Part A, 26 (1994) 237-252.

[3] S.A. Logtenberg, M. Nijemeisland, A.G. Dixon, Computational fluid dynamics simulations of fluid flow and heat transfer at the wall-particle contact points in a fixed bed reactor, *Chemical Engineering Science*, 54 (1999) 2433-2439.

[4] S.A. Logtenberg, A.G. Dixon, Computational fluid dynamics studies of fixed bed heat transfer, *Chemical Engineering and Processing*, 37 (1998) 7-21.

[5] S.J.P. Romkes, F.M. Dautzenberg, C.M. Van Den Bleek, H.P.A. Calis, CFD modelling and experimental validation of particle-to-fluid mass and heat transfer in a packed bed at very low channel to particle diameter ratio, *Chemical Engineering Journal*, 96 (2003) 3-13.

[6] P. Magnico, Hydrodynamic and transport properties of packed beds in small tube-to-sphere diameter ratio: pore scale simulation using an Eulerian and a Lagrangian approach, *Chemical Engineering Science*, 58 (2003) 5005-5024.

[7] A. Guardo, M. Coussirat, M.A. Larrayoz, F. Recasens, E. Egusquiza, Influence of the turbulence model in CFD modelling of wall-to-fluid heat transfer in packed beds, *Chemical Engineering Science*, 60 (2005) 1733-1742.

[8] A. Guardo, M. Coussirat, F. Recasens, M.A. Larrayoz, X. Escaler, CFD on particle-to-fluid heat transfer in fixed bed reactors: Convective heat transfer at low and high pressure, *Chemical Engineering Science*, 61 (2006) 4341-4353.

[9] A.A. Merrikh, J.L. Lage, Natural convection in an enclosure with disconnected and conducting solid blocks, *International Journal of Heat and Mass Transfer*, 48 (2005) 1361-1372.

[10] T. Norton, D.W. Sun, Computational fluid dynamics (CFD) – an effective and efficient design and analysis tool for the food industry: A review, *Trends in Food Science & Technology*, 17 (2006) 600-620.

[11] S.A. Tassou, W. Xiang, Modelling the environment within a wet air-cooled vegetable store, *Journal of Food Engineering*, 38 (1998) 169-187.

[12] Q. Zou, L. Opara, R. McKibbin, A CFD modeling system for airflow and heat transfer in ventilated packaging for fresh foods: I. Initial analysis and development of mathematical models, *Journal of Food Engineering*, 77 (2006) 1037-1047.

[13] Q. Zou, L. Opara, R. McKibbin, A CFD modeling system for airflow and heat transfer in ventilated packaging for fresh foods: II. Computational solution, software development and model testing, *Journal of Food Engineering*, 77 (2006) 1048-1058.

[14] H.B. Nahor, M.L. Hoang, P. Verboven, M. Baelmans, B.M. Nicolai, CFD model of the air flow, heat and mass transfer in cool stores, *International Journal of Refrigeration*, 28 (2005) 368-380.

[15] M. Quintard, S. Whitaker, Transport in ordered and disordered porous media I : the cellular average and the use of weighting functions, *Transport in Porous Media*, 14 (1994-a) 163-177.

[16] M. Quintard, S. Whitaker, Transport in ordered and disordered porous media II : generalized volume averaging, *Transport in Porous Media*, 14 (1994-b) 179-206.

[17] M. Kaviany, *Principles of Heat Transfer in Porous Media*, Mechanical Engineering Series, Springer-Verlag, New York, 1991.

[18] R.B. Bird, W.E. Stewart, E.N. Lightfoot, *Transport Phenomena*. Ed. John Wiley, 1960.

[19] R.G. Carbonell, S. Whitaker, Heat and mass transfer in porous media, In *Fundamentals of Transport Phenomena in Porous Media*, Ed. Bear and Corapcioglu, Martinus Nijhoff, 1984, pp. 121-198.

[20] N. Wakao, S. Kaguei, *Heat and Mass Transfer in Packed Bed*, Gordon and Breach Science, New York, 1982, 408p.

[21] D.J. Tanner, A.C. Cleland, L.U. Opara, T.R. Robertson, A generalised mathematical modelling methodology for design of horticultural food packages exposed to refrigerated conditions: Part 1, Formulation, *International Journal of Refrigeration*, 25 (2002) 33-42.

[22] D.J. Tanner, A.C. Cleland, L.U. Opara, T.R. Robertson, A generalised mathematical modelling methodology for design of horticultural food packages exposed to refrigerated conditions: Part 2, Heat transfer modelling and testing, *International Journal of Refrigeration*, 25 (2002) 43-53.

[23] Kaguei S., Shiozawa B., Wakao N., Dispersion-Concentric model for packed bed heat transfer, *Chemical Engineering Science*, 32 (5) (1976) 507-513.

[24] G.E. Mueller, A heat transfer model for volumetrically heated nuclear debris beds, Nuclear Engineering and Design, 98 (1) (1986) 1-8.

[25] Y. Xu, D. Burfoot, Simulating the bulk storage of foodstuffs, *Journal of Food Engineering*, 39 (1999) 23-29.

[26] S. Ergun, Fluid Flow Through Packed Columns, *Chemical Engineering Progress*, 48 (2) (1952) 89-94.

[27] E. Achenbach, Heat and Flow Characteristics of Packed Bed, *Experimental Thermal and Fluid Science*, 10 (1995) 17-27.

[28] S. Ben Amara, Ecoulements et transferts thermiques en convection naturelle dans les milieux macroporeux alimentaires: Application aux réfrigérateurs ménagers, Thèse doctorat de l'Institut National de Paris-Grignon, 2005.

[29] S. Ben Amara, O. Laguerre, D. Flick, Experimental study of convective heat transfer during cooling with low air velocity in a stack of objects, *International Journal of Thermal Sciences*, 43, (2004) 1212-1221.

[30] O. Laguerre, S. Ben Amara, D. Flick, Heat transfer between wall and packed bed crossed by low velocity airflow. *Applied Thermal Engineering*, 26 (2006) 1951-1960.

[31] E. H. Chui, G. D. Raithby, Computation of radiant heat transfer on a non-orthogonal mesh using the finite-volume method. *Numerical Heat Transfer*, Part B, 23 (1993) 269-288.

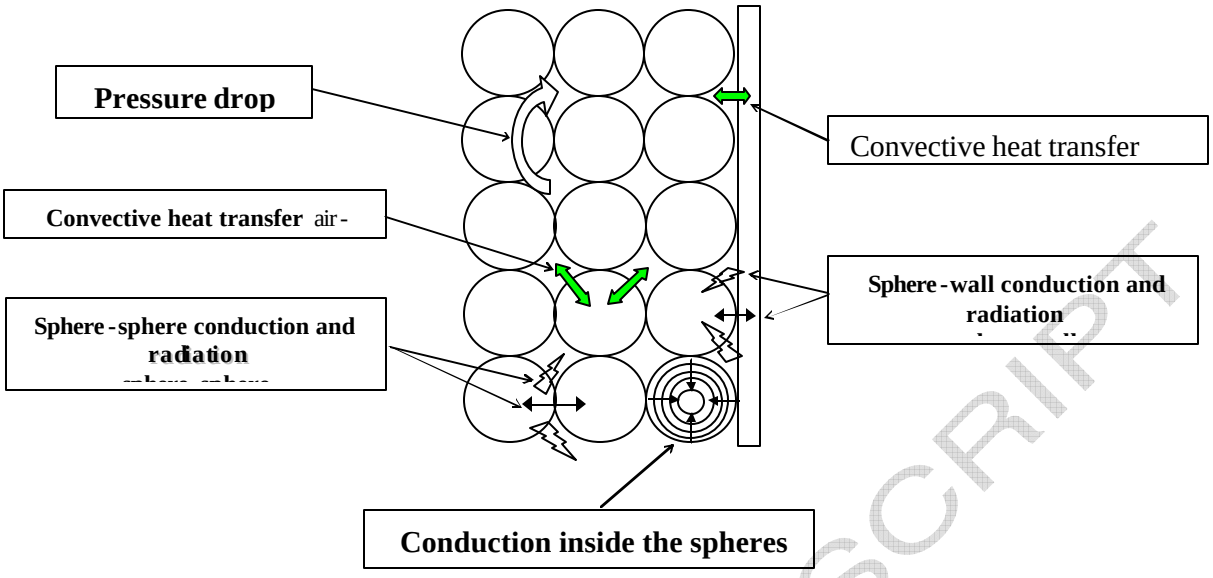

Figure 1. Different heat transfer modes and momentum transfer taken into account in the packed bed modeling approach.

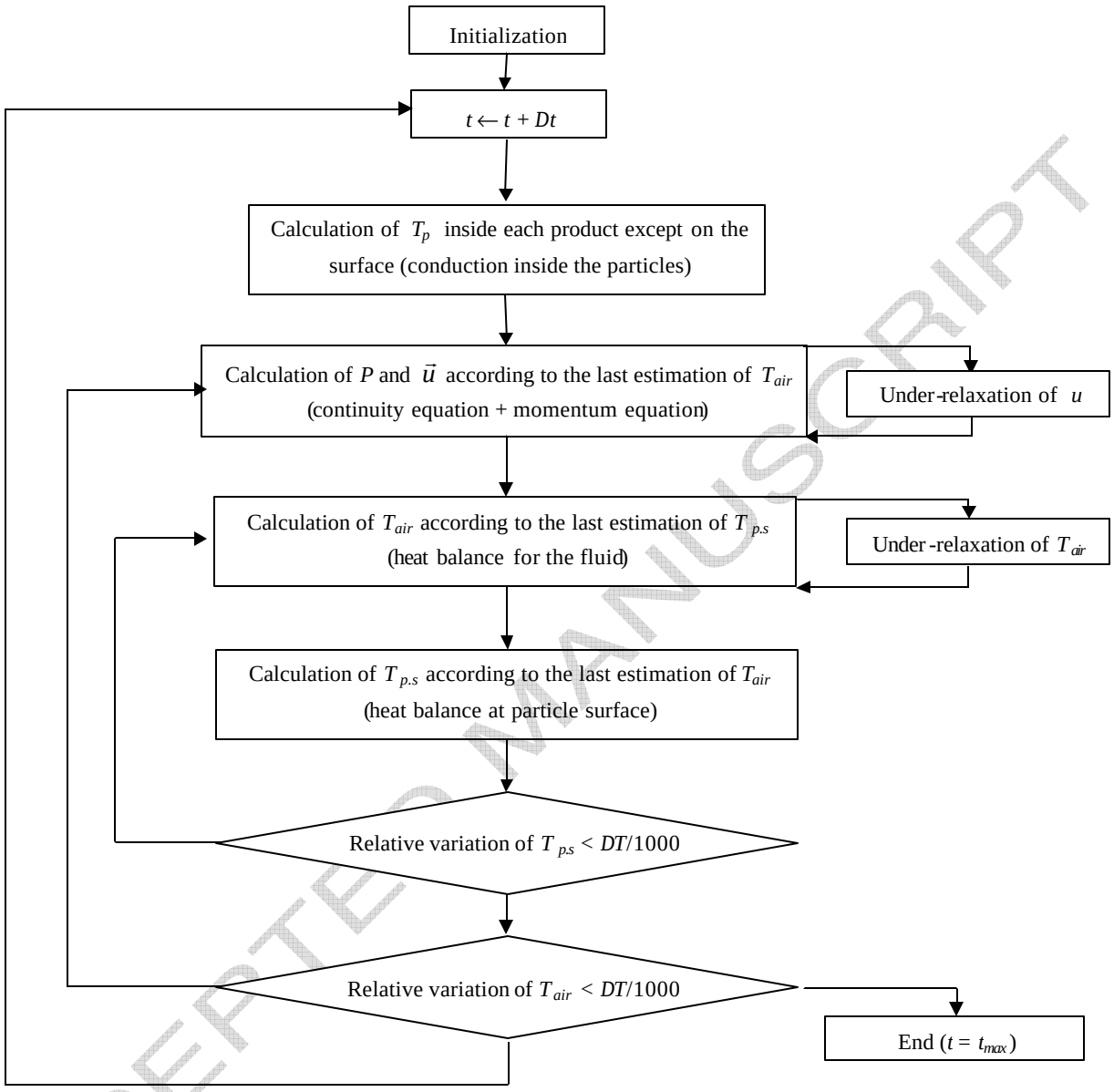

Figure 2. General algorithm of the numerical resolution (DT is a characteristic temperature difference, e.g. the difference between initial and final product temperatures)

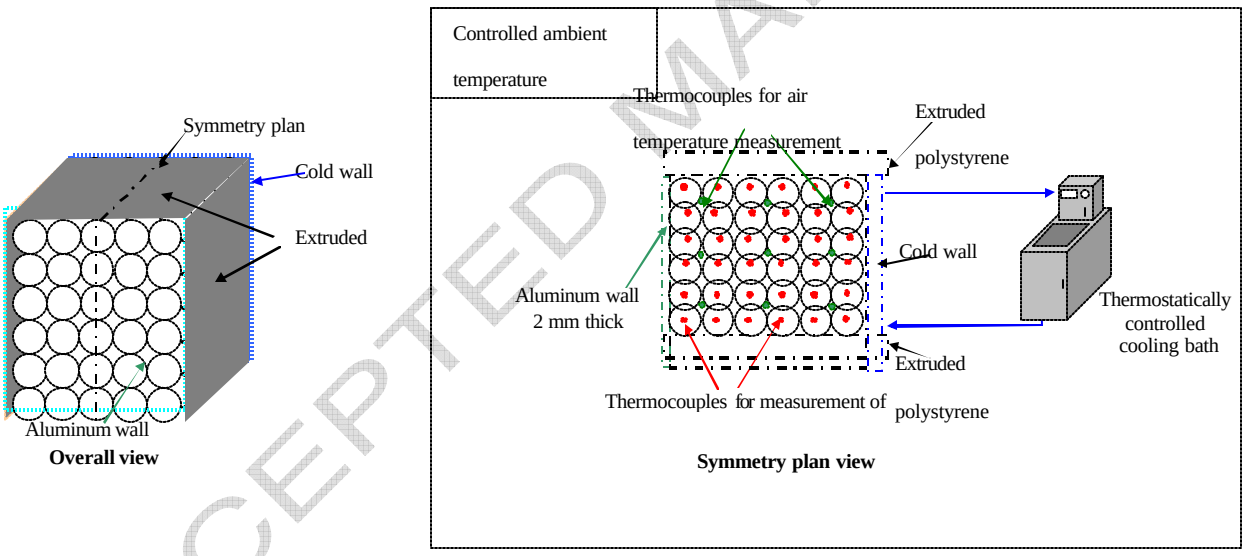

Figure 3. Experimental device consisting of a stack of spheres (PVC spheres filled with gelatin gel, diameter 7.5 cm) arranged in an insulated box (except two vertical aluminum walls maintained at 0°C and 30°C).

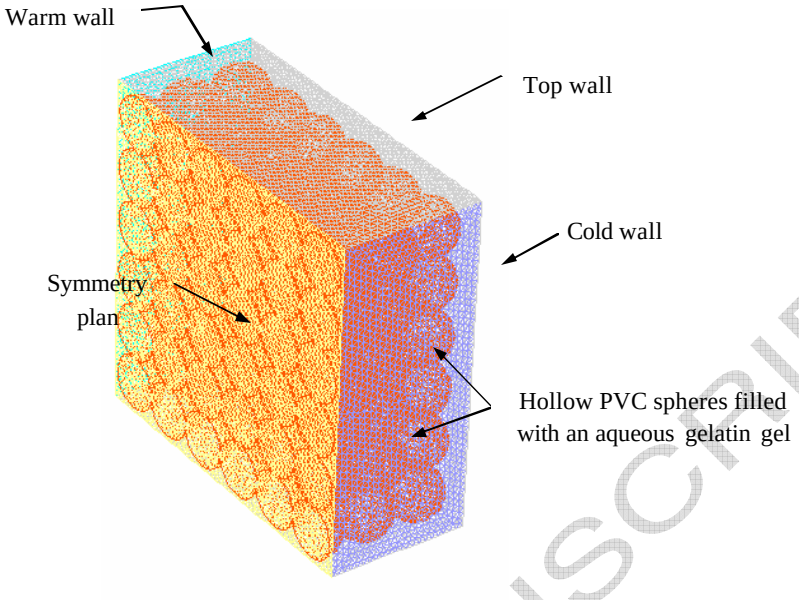

Figure 4. Mesh structure (189,124 cells for solid spheres and 214,495 cells for air).

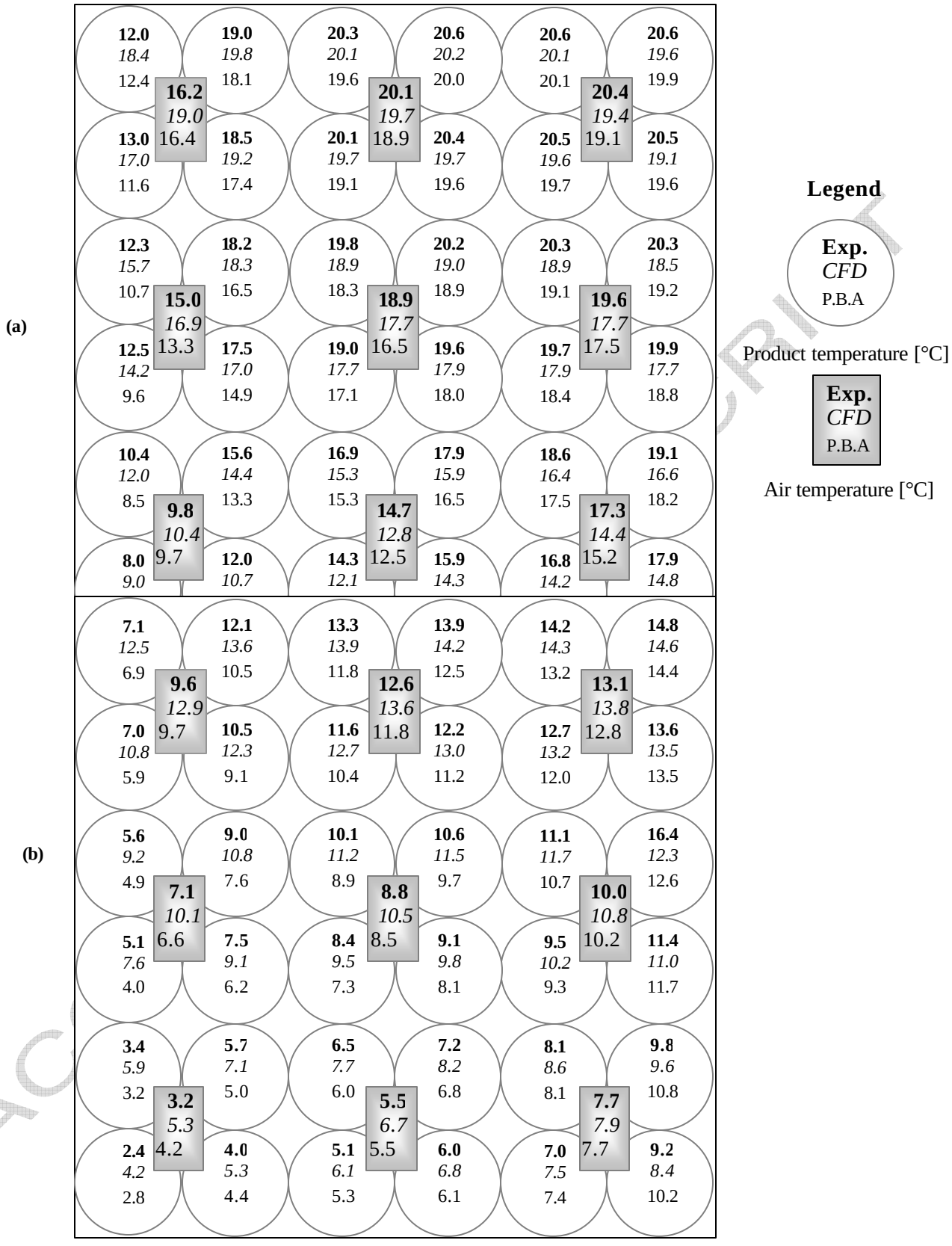

Figure 5. Measured and predicted product and air temperatures, (a) After 500 min; (b) After 10 000 min.(P.B.A= Packed Bed Approach).

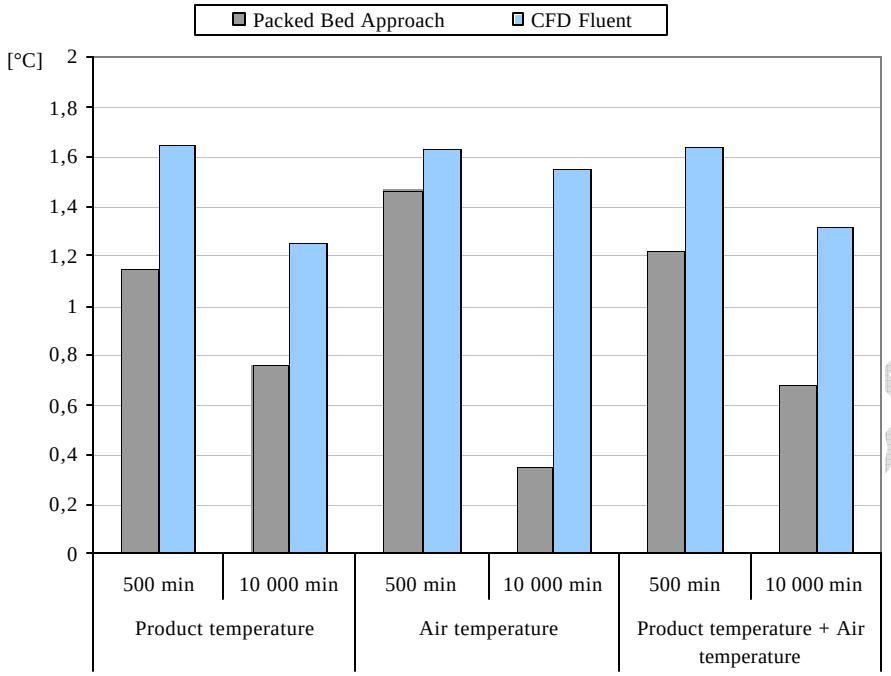

Figure 6 Mean error of prediction $\overline{|T_{measured} - T_{predicted}|}$ for air temperature and solid temperature at the centre of the spheres.

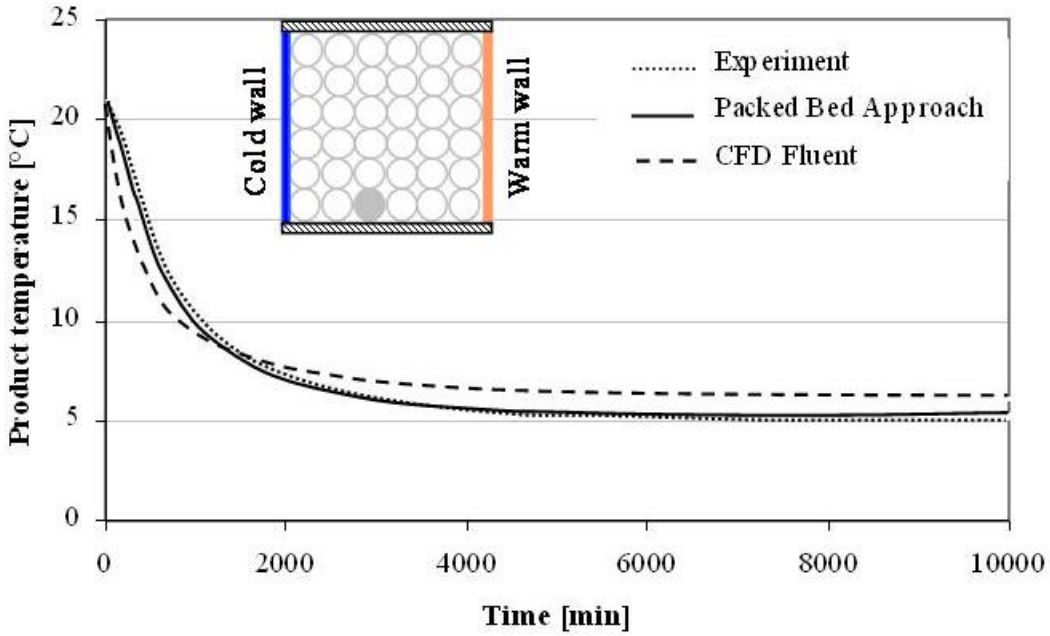

(a)

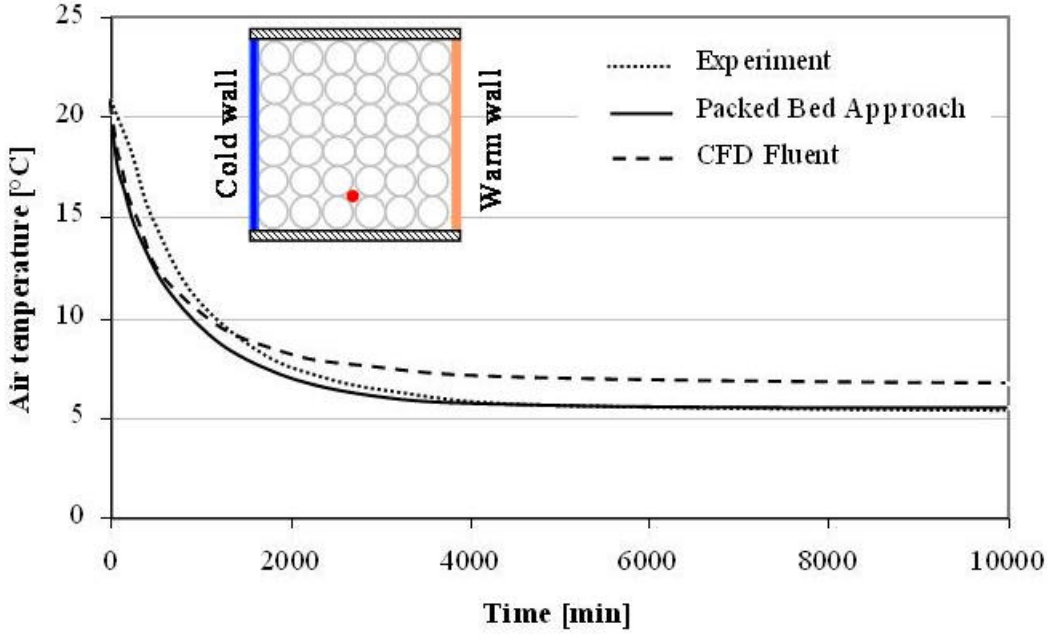

(b)

Figure 7. Example of a comparison between experimental product/air temperature evolution and calculated values obtained by packed bed and CFD Fluent approaches.

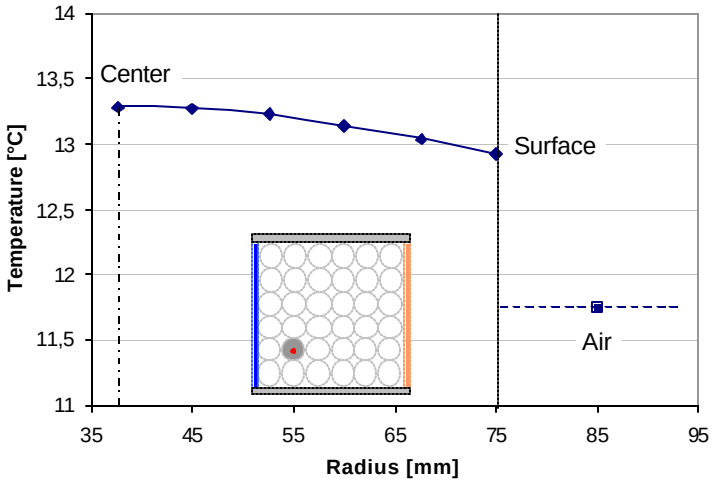

Figure 8. Example of temperature variation between the centre and the surface of a sphere predicted by the packed bed approach (after 500 min).

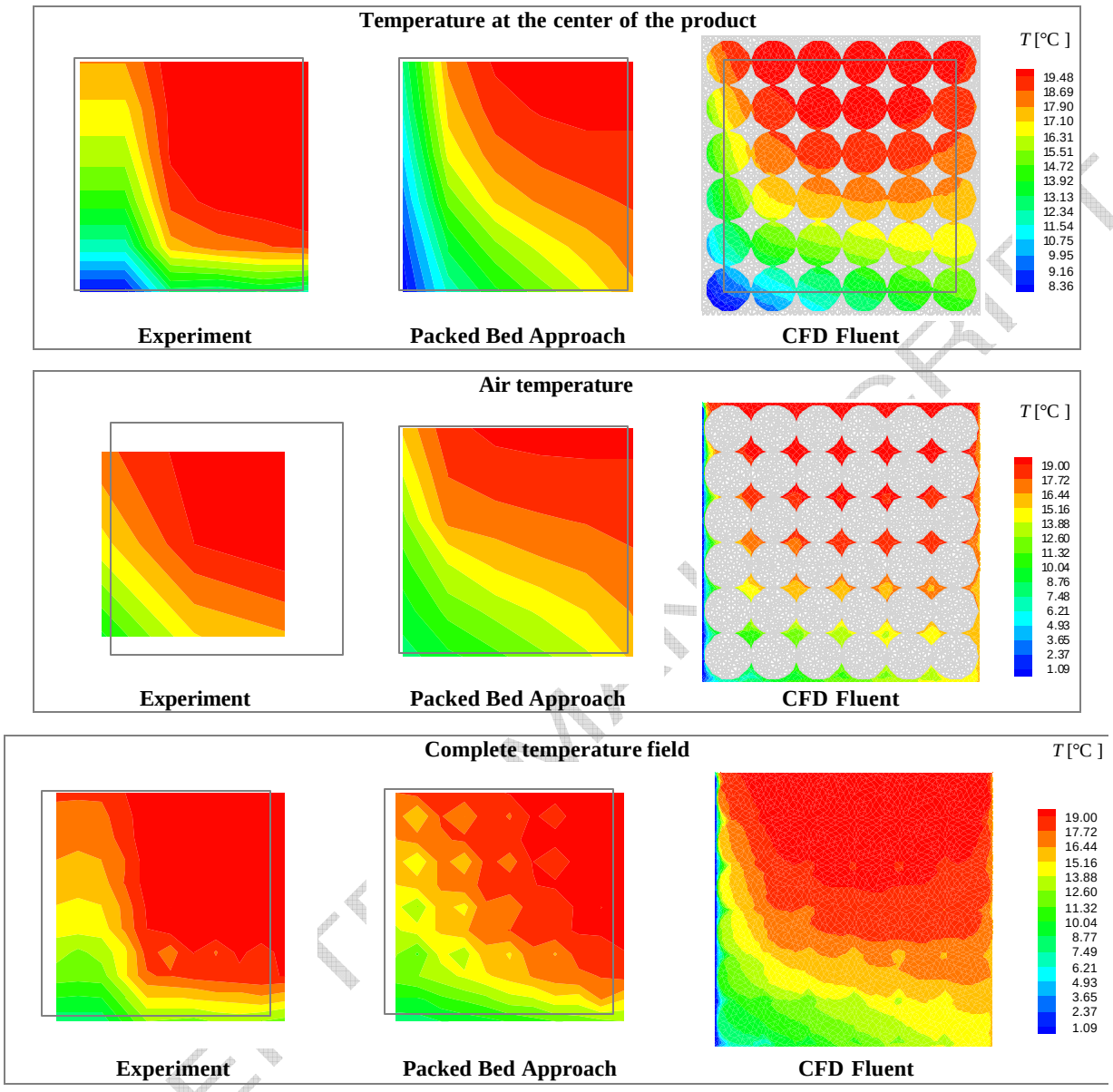

Figure 9. Experimental and numerical temperature fields on the symmetry plan after 500 min.
The experimental values obtained at the measurement points (Fig. 3) were interpolated (by Tecplot) to present product and air temperature fields. For the "complete temperature field", product temperature is assigned to the position of the sphere centers and the air temperature to the position of void space centers. The same method is used for the packed bed approach from the values obtained at the mesh nodes. The CFD approach gives directly the temperature fields.

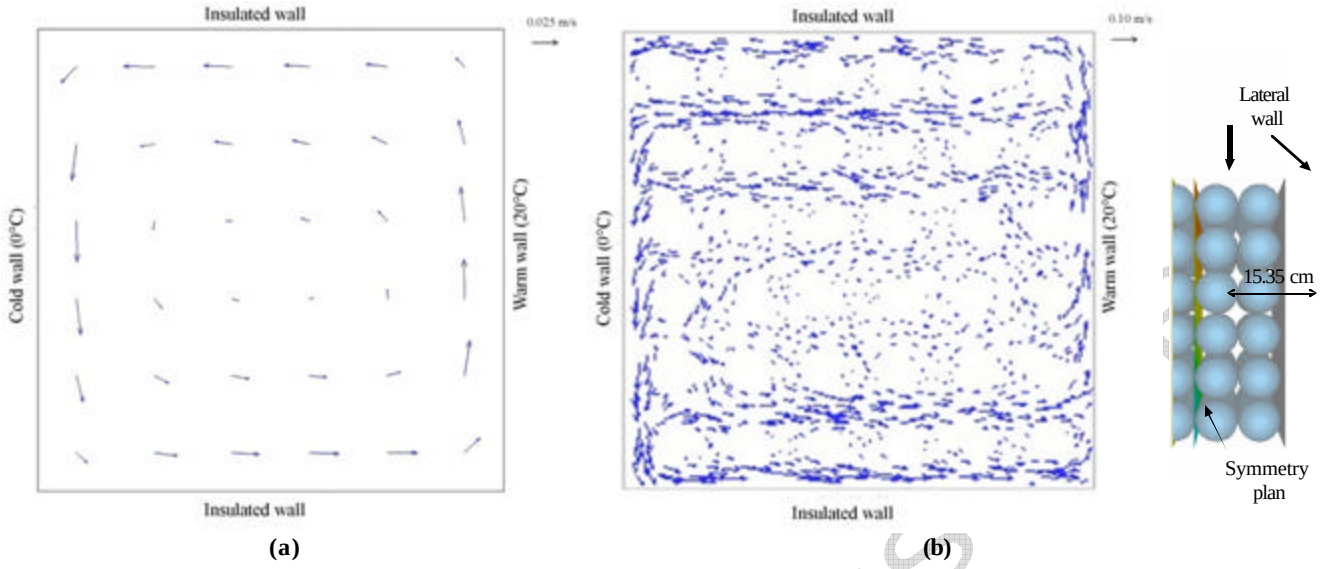

Figure 10. Predicted velocity fields when steady state is reached, (a) Packed Bed Approach; (b) CFD Fluent (on the plan situated at 15.35 cm from the side wall).

Table 1. Main Solving Parameters

Variable	Under Relaxation Factor	Discretization
Pressure (continuity)	0.8	Presto
Momentum	0.2	Second order upwind
Energy	1	Second order upwind
Pressure/momentum coupling	-	Simple